

Deuterium exchange of α -helices and β -sheets as monitored by electrospray ionization mass spectrometry

DAVID S. WAGNER,¹ LAURA G. MELTON,² YIBING YAN,² BRUCE W. ERICKSON,² AND ROBERT J. ANDEREGG¹

¹ Glaxo Research Institute, Research Triangle Park, North Carolina 27709

² Department of Chemistry, University of North Carolina at Chapel Hill, Chapel Hill, North Carolina 27599-3290

(RECEIVED March 15, 1994; ACCEPTED May 20, 1994)

Abstract

Deuterium exchange was monitored by electrospray ionization mass spectrometry (ESI-MS) to study the slowly exchanging (hydrogen bonded) peptide hydrogens of several α -helical peptides and β -sheet proteins. Polypeptides were synthetically engineered to have mainly disordered, α -helical, or β -sheet structure. For 3 isomeric 31-residue α -helical peptides, the number of slowly exchanging hydrogens as measured by ESI-MS in 50% $\text{CF}_3\text{CD}_2\text{OD}$ (pD 9.5) provided estimates of their α -helicities (26%, 40%, 94%) that agreed well with the values (17%, 34%, 98%) measured by circular dichroic spectroscopy in the same nondeuterated solvent. For 3 betabellins containing a pair of β -sheets and a related disordered peptide, their order of structural stability (12D > 12S > 14D > 14S) shown by their deuterium exchange rates in 10% $\text{CD}_3\text{OD}/0.5\% \text{CD}_3\text{CO}_2\text{D}$ (pD 3.8) as measured by ESI-MS was the same as their order of structural stability to unfolding with increasing temperature or guanidinium chloride concentration as measured by circular dichroic spectroscopy in water. Compared to monitoring deuterium exchange by proton NMR spectrometry, monitoring deuterium exchange by ESI-MS requires much less sample (1–50 μg), much shorter analysis time (10–90 min), and no chemical quenching of the exchange reaction.

Keywords: betabellin; deuterium exchange; electrospray ionization; helical peptides; mass spectrometry; protein engineering; secondary structure

The rate of deuterium exchange of peptide amide hydrogens provides a useful probe of protein structure. Deuterium exchange as monitored by proton NMR spectroscopy has been used to determine protein conformations (Wagner & Wüthrich, 1982; Jeng et al., 1990; Englander & Mayne, 1992), protein structural fluctuations (Rosa & Richards, 1979; Rohl et al., 1992), protein folding intermediates (Dobson & Evans, 1988; Bycroft et al., 1990), the effects of ligands, inhibitors, and substrates on enzymes (Brandt & Woodward, 1987; Paterson et al., 1990; Mayne et al., 1992), and the exchange kinetics of peptide backbone amide hydrogens (Hvidt & Nielsen, 1966; Molday et al., 1972; Woodward et al., 1982; Creighton, 1984, 1990; Roder et al., 1985). Many peptide backbone amide hydrogens in proteins are rapidly exchanged by deuteriums at rates similar to those for amide hydrogens in small model compounds, indicating that they are near the protein surface and readily accessible to water. Other peptide backbone amide hydrogens exchange more slowly, indicating that they are involved in intramolecular hydrogen bonds

and/or are less accessible to water. The number of slowly exchanging hydrogens and their rates of deuterium exchange depend on such factors as pH, temperature, pressure, charge, chemical environment, and 3-dimensional protein structure (Englander et al., 1972; Woodward & Hilton, 1979; Kim & Baldwin, 1982; Mathew & Richards, 1983; Englander & Kallenback, 1984; Perrin & Lollo, 1984). Proton NMR studies have revealed that most slowly exchanging hydrogens are hydrogen bonded backbone amide hydrogens of secondary structural elements such as α -helices and β -sheets. In order for deuterium exchange to occur, the hydrogen bond must be broken, which may require several small unfolding steps. Thus, the deuterium exchange rate of a hydrogen bonded backbone amide hydrogen is related to the free energy of its local secondary structure.

Electrospray ionization (ESI) is a relatively gentle mass spectrometry (MS) technique for producing gas phase ions from an analyte solution (Covey et al., 1988; Fenn et al., 1990). Performed at atmospheric pressure and room temperature, ESI is useful for mass spectral analysis of proteins and other large biomolecules, for which it produces mainly multiply charged molecular ions. Each charge state provides an independent measure

Reprint requests to: Robert J. Anderegg, Glaxo Research Institute, Five Moore Drive, Research Triangle Park, North Carolina 27709.

of the molecular mass of the protein, once the charge is known. A protein with a high molecular mass can be analyzed if the mass:charge (m/z) ratios of its molecular ions in several charge states are within the detectable range.

ESI-MS has been used to study changes in protein conformation (LeBlanc et al., 1991; Mirza et al., 1993; Wagner & Anderegg, 1994). When a protein is analyzed under denaturing conditions, the higher charge states become more abundant. As a protein is denatured, more of its functional groups become charged and electrostatically repelled by other groups of like charge, which produces higher charge states that are observed at lower m/z ratios. Mass spectrometry has also been used in conjunction with deuterium exchange (Katta & Chait, 1991; Thevenon-Emeric et al., 1992; Miranker et al., 1993; Stevenson et al., 1993; Zhang & Smith, 1993). The number of deuteriums incorporated and the average rates of deuterium exchange are easily measured through the increase in the molecular mass with time. Deuterium exchange rates are usually faster for a protein under denaturing conditions than under nondenaturing conditions because a loosely folded structure exchanges faster than a tightly folded structure.

We have used ESI-MS to monitor the deuterium exchange of 7 synthetic peptides and proteins designed to have mainly disordered, α -helical, or β -sheet structure. These compounds are simple models of more complex protein structures. For 3 α -helical peptides, the number of slowly exchanging hydrogens at pD 9.5 as measured by ESI-MS provided estimates of their α -helicities that agreed well with their α -helicities as measured by circular dichroic spectroscopy. For 3 β -sheet proteins and a related disordered peptide, deuterium exchange rates at pD 3.8 for discrete sets of slowly exchanging hydrogens as measured by ESI-MS provided an order of structural stability that was the same as their order of structural stability to unfolding with increasing temperature or guanidinium chloride concentration as measured by CD spectroscopy.

Results and discussion

α -Helical peptides

Design

Three isomeric 31-residue single-chain peptides were engineered as models of α -helical structures (Fig. 1). Peptides E8A, E8B, and E8C each had the composition Glu₈ Leu₈ Ala₁₄ Asp and contained 10 carboxyl groups and 1 amino group. Glutamic acid, leucine, and alanine residues were used because they favor formation of an α -helix (Chou & Fasman, 1974).

The α -helicity of these peptides should be influenced by the locations of the ionizable glutamic acid residues. At a pH >5, several glutamic acid residues are mutually repelled due to their

common negative charges. The charge repulsion of 2 covalently linked glutamates (Glu⁻-Glu⁻) should have little influence on α -helicity because they are nearly the same distance apart in either the α -helical or extended conformation. The charge repulsion of 2 conformationally adjacent glutamates, such as Glu⁻-X-X-X-Glu⁻ in an α -helix, should significantly influence α -helicity because these glutamates are much closer together in the α -helical conformation than in the extended conformation. During the folding of an α -helix, a pair of glutamates separated by 2-3 other residues are brought close together on adjacent helical turns. The folding energy of this α -helix should be significantly higher than that of an isomeric α -helix having the pair of glutamates separated by 5-7 other residues, which places them on the same side of the α -helix but separated by a third turn.

The geometric relationships of the Glu residues are illustrated by the α -helical nets for peptides E8A, E8B, and E8C (Fig. 2). E8A contained 3.75 adjacent copies of the octad Ala-Glu-Leu-Ala-Leu-Glu-Ala-Ala, with the Glu residues separated by 3 residues. Similarly, E8B contained the octad Glu-Glu-Leu-Ala-Leu-Ala-Ala-Ala, in which the underlined alanine and glutamic acid residues were reversed from E8A and the Glu-Glu pairs are separated by 6 residues (Fig. 1). The fully α -helical form of E8A would have all 8 Glu residues held close together to form a polyanionic strip down the side of the helix. A negatively charged glutamate in the middle of this strip could be repelled by the negative charge of a glutamate on the preceding helical turn and by another on the following turn. Although E8A and E8B had identical residues at 23 (74%) of their 31 positions, E8A should have significantly lower α -helicity than E8B due to charge repulsions between the Glu residues. E8C, however, contained 4 adjacent copies of the heptad Leu-Glu-Glu-Leu-Ala-Ala-Ala, with the Glu-Glu pairs separated by 5 residues. Additionally, all 8 leucines were placed at the first or fourth position of the heptad, which is typical of an α -helical coiled-coil (Fig. 1). Under physiological conditions, the 2 hydrophobic faces of 2 chains of E8C should form a stable noncovalent dimer. At pH 7.4, 2 molecules of peptide E8C formed a stable 2-stranded parallel α -helical coiled-coil that had a $[\theta]_{222}/[\theta]_{208}$ ratio of 0.97 at 25 °C (Melton et al., 1994).

CD spectroscopy

Peptides E8A, E8B, and E8C were separately dissolved in 1:1 (v/v) CF₃CH₂OH/H₂O and adjusted to pH 9.5 by addition of NH₄OH. Their CD spectra (Fig. 3) displayed a minimum near 222 nm and a stronger minimum near 208 nm, which is diagnostic of α -helical structure. The α -helicity calculated from $[\theta]_{222}$ was 17% for E8A, 34% for E8B, and 98% for E8C. Peptide E8A exhibited only half the α -helicity of peptide E8B, and both peptides were mainly disordered, which was consistent with their structural designs. As shown by its $[\theta]_{222}/[\theta]_{208}$ ratio of 0.79,

	1	5	10	15	20	25	30	32																												
12	H	T	L	T	A	S	I	p	d	L	T	S	I	N	p	d	T	A	T	C	K	V	p	d	F	T	L	S	I	G	A					
14	H	S	L	T	A	S	I	k	a	L	T	I	H	V	Q	a	k	T	A	T	C	Q	V	k	a	Y	T	V	H	I	S	E				
E8A	D	<u>A</u>	<u>E</u>	<u>L</u>	<u>A</u>	<u>L</u>	<u>E</u>	<u>A</u>	<u>A</u>	<u>A</u>	<u>E</u>	<u>L</u>	<u>A</u>	<u>L</u>	<u>E</u>	<u>A</u>	<u>A</u>	<u>A</u>	<u>E</u>	<u>L</u>	<u>A</u>	<u>L</u>	<u>E</u>	<u>A</u>	<u>A</u>	<u>E</u>	<u>L</u>	<u>A</u>	<u>L</u>	<u>E</u>	<u>A</u>					
E8B	D	<u>E</u>	<u>E</u>	<u>L</u>	<u>A</u>	<u>L</u>	<u>A</u>	<u>A</u>	<u>A</u>	<u>E</u>	<u>E</u>	<u>L</u>	<u>A</u>	<u>L</u>	<u>A</u>	<u>A</u>	<u>A</u>	<u>E</u>	<u>E</u>	<u>L</u>	<u>A</u>	<u>L</u>	<u>A</u>	<u>A</u>	<u>E</u>	<u>L</u>	<u>A</u>	<u>L</u>	<u>E</u>	<u>A</u>	<u>L</u>	<u>E</u>	<u>A</u>			
E8C	D	<u>L</u>	<u>E</u>	<u>E</u>	<u>L</u>	<u>A</u>	<u>A</u>	<u>A</u>	<u>L</u>	<u>E</u>	<u>E</u>	<u>L</u>	<u>A</u>	<u>A</u>	<u>A</u>	<u>L</u>	<u>E</u>	<u>E</u>	<u>L</u>	<u>A</u>	<u>L</u>	<u>A</u>	<u>A</u>	<u>L</u>	<u>E</u>	<u>E</u>	<u>L</u>	<u>A</u>	<u>A</u>	<u>A</u>	<u>L</u>	<u>E</u>	<u>A</u>	<u>L</u>	<u>E</u>	<u>A</u>

Fig. 1. Amino acid sequences of the 5 peptide chains of the β -sheet proteins betabellin 12S, 12D (represented by 12), and 14D, the disordered peptide betabellin 14S (represented by 14), the partially α -helical peptides E8A and E8B, and the 2-stranded α -helical coiled-coil protein E8C (a, D-Ala; d, D-Asp; k, D-Lys; p, D-Pro; heptads are double underlined and octads are single underlined).

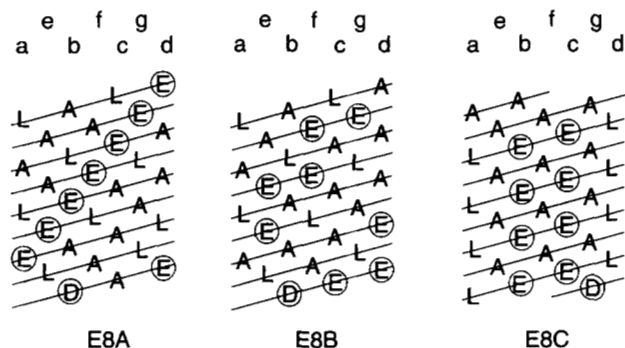


Fig. 2. Helical net representations of peptide chains E8A, E8B, and E8C showing the distribution of acidic residues (circled).

peptide E8C was monomeric in 50% trifluoroethanol at pH 9.5 because trifluoroethanol destabilizes the coiled-coil dimer but maintains the α -helicity of the monomeric peptide chains (Hodges et al., 1988).

Electrospray ionization mass spectrometry

Peptides E8A, E8B, and E8C each contained 9 acidic but no basic residues and were insoluble below pH 7, so negative ionization was used for their mass spectral analysis. Because they had the same amino acid composition, they gave similar mass spectra. As illustrated for E8C in Figure 4, the mass spectrum displayed peaks for the -2 (m/z 1,532.3), -3 (m/z 1,021.1), and -4 (m/z 765.7) charged states, giving a measured molecular mass of 3,066.6 Da, consistent with the calculated average mass (3,066.4 Da).

The uncharged state of each of these 31-residue peptide chains contained 42 exchangeable hydrogens (NH_2 [N-terminus], 30 $\text{O}=\text{C}-\text{N}-\text{H}$, CO_2H [C-terminus], 8 Glu CO_2H , 1 Asp CO_2H).

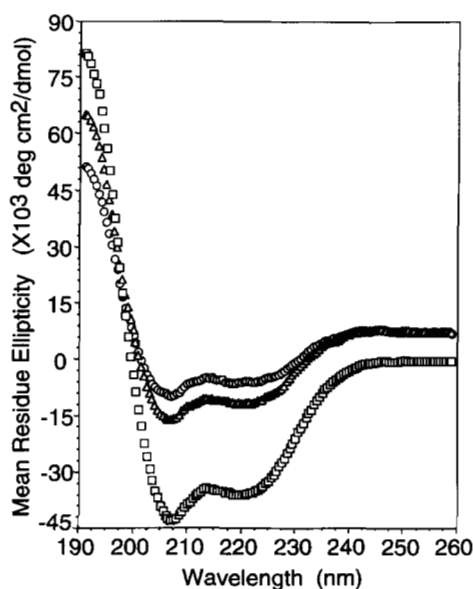


Fig. 3. Circular dichroic spectra of the peptides E8A (O), E8B (Δ), and E8C (\square) dissolved at a concentration of 40 μM in 1:1 $\text{CF}_3\text{CH}_2\text{OH}/\text{H}_2\text{O}$ (pH 9.5).

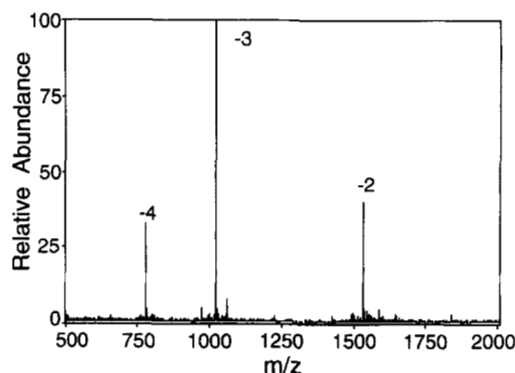


Fig. 4. Negative-ion electrospray ionization mass spectrum of E8C in 1:1 $\text{CF}_3\text{CH}_2\text{OH}/\text{H}_2\text{O}$ (pH 9.5).

In the fully α -helical conformation, 27 of the 30 backbone amide hydrogens would participate in an i to $i-4$ hydrogen bond ($\text{N}-\text{H}\cdots\text{O}=\text{C}$), in which the main-chain $\text{N}-\text{H}$ hydrogen of residue i interacts electrostatically with the main-chain $\text{C}=\text{O}$ oxygen of residue $i-4$. During deuterium exchange, the molecular mass should increase from 3,066 Da before exchange to 3,108 Da after complete exchange.

Lyophilized samples of E8A, E8B, and E8C were separately dissolved in 1:1 (v/v) $\text{CF}_3\text{CD}_2\text{OD}/\text{D}_2\text{O}$ and adjusted to pH 9.5 by addition of ND_4OD . The ESI-MS data for peptides E8A, E8B, and E8C are shown in Figure 5A for the first 8 min and in Figure 5B for 0.15–0.35 min after deuterium exchange began. In general, the deuterium exchange data obtained from ESI-MS can be plotted as molecular mass versus time. However, a more useful plot is the number of remaining exchangeable hydrogens (H_t) with time. The fully deuterated molecular mass can be easily calculated by adding 1 Da for every exchangeable hydrogen. The number of remaining hydrogens (H_t) at each time point t can be determined by subtracting the molecular mass at time point t from the fully deuterated molecular mass. The data in Figure 5 show the deuterium exchange was significantly faster for E8A (17% α -helicity by CD) and E8B (34% α -helicity by CD) than for E8C (98% α -helicity by CD).

At pH 9.5, the backbone amide exchange rates are at least 100 times slower than those at all other labile sites (Wüthrich, 1986). Because the exchange rate is catalyzed by both acid and base, amide exchange rates follow a U-shaped curve with a minimum around pH 3. Each pH unit away from the minimum increases the rate 10-fold. Thus, at pH 9.5, all labile hydrogens not involved in intramolecular bonding are expected to exchange very quickly (before mass spectral detection). The first 4 amides in an α -helix do not hydrogen bond because they have no carbonyl partner; therefore, they experience a faster rate of exchange. After accounting for all of the fast exchanging hydrogens, a total of 27 remaining hydrogens can be involved in hydrogen bonding, and may exchange on a slower time scale. The relative slowness of the exchange curves represented in Figure 5 is due to the amide hydrogens involved in the helix hydrogen bonding network because the hydrogen bond must be broken in order for exchange to occur.

An exchangeable hydrogen should exhibit apparent first-order kinetics. A set of hydrogens that undergo deuterium exchange at the same rate should obey the equation $\ln(H_t) = \ln(H_n) - kt$,

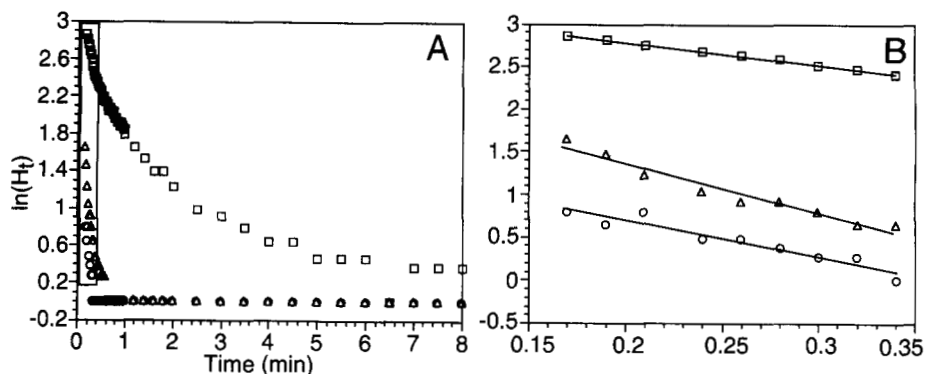


Fig. 5. Time-dependent decrease in the number of exchangeable hydrogens remaining (H_t) in peptides E8A (○), E8B (△), and E8C (□) during the first 8 min (A) and the first 0.35 min (B) following exposure to deuterated solvents (1:1 $\text{CF}_3\text{CD}_2\text{OD}/\text{D}_2\text{O}$, pD 9.5). Box in A is the region expanded in B.

where H_t is the number of unexchanged hydrogens at time t , H_n is the number of exchangeable hydrogens in the set n , and k is the apparent first-order rate constant for the set. Plots of $\ln(H_t)$ as a function of time can produce 1 or more linear segments along the exchange curve, each representing a set of hydrogens exchanging at the same apparent first-order rate. In order to convert the linear segments along the exchange curve from the plots of $\ln(H_t)$ versus t into kinetic quantities, the following general scheme was employed. For a hypothetical data set shown in Figure 6, 4 linear segments are observed. Linear regression is applied on each segment to define the best straight line fit of the data and to determine the intercept, slope, and their associated errors. The apparent endpoints of each segment are determined by visual inspection. The intercept (I_n) of any

line represents the natural logarithm of the sum of the number of hydrogens in set n , represented by the line, and in all sets of slower exchanging hydrogens. The population for all hydrogens experiencing the same first-order kinetics (H_n) of set n is

$$H_n = e^{I_n} - e^{I_{n+1}}.$$

A set of hydrogens (H_1) exchanges so fast that their rates are not measurable using our method. The population of this set is $H_1 = H_0 - e^{I_2}$, where H_0 represents the total number of exchangeable hydrogens in the peptide. Although the exchange rates of the H_1 hydrogens cannot be measured, we can put a lower limit on the rate. Because all the hydrogens in this set have exchanged by the time we measure our first time point (12 s), we assume that 12 s represents at least 4 half-lives (94% would exchange in 4 half-lives). The exchange rates must, therefore, be greater than 0.23 s^{-1} . The populations of sets 2–5 are determined as above, and their exchange rates are derived directly from the slopes of the regression lines. Set 6 hydrogens exchange too slowly to be measured in the time frame of the experiment and are represented by the number of hydrogens not exchanged after the last data point collected, i.e., at 13 min. The exchange rate of these slowly exchanging hydrogens must be less than or equal to the rate of the last linear segment, representing set 5. The linear segment may continue beyond where we stopped measuring ($k_6 = k_5$) or yet another linear segment of smaller slope may exist, but we have not sampled from it ($k_6 < k_5$).

Plotting the $\ln(H_t)$ versus time for the 3 helical peptides for the first 10-s period of data acquisition gave a straight line for each peptide (Fig. 5B). The linear regression coefficient was 0.97 for E8A, 0.98 for E8B, and 0.99 for E8C. In this brief time period, each peptide behaved as if it contained a set of hydrogens (H_2) that were undergoing deuterium exchange at essentially the same rate. Beyond 0.35 min, peptides E8A and E8B are completely exchanged. The apparent first-order rate constant for each of the sets, obtained from the slope of each line, was 0.098 s^{-1} for E8A and E8B and 0.043 s^{-1} for E8C. From the y -intercepts of the plot, the number of hydrogens in the set was calculated to be 4.0 for E8A, 8–9 for E8B, and 25 for E8C. During this 10-s period, E8A had a set of 4 H and E8B had a set of 8–9 H that were undergoing first-order deuterium exchange at the rate of one every 10 s. E8C contained a set of 25 H undergoing exchange at approximately half that rate. Because the slope of the data for E8C in Figure 5A, however, became less negative with increasing time, many of these 25 H actually un-

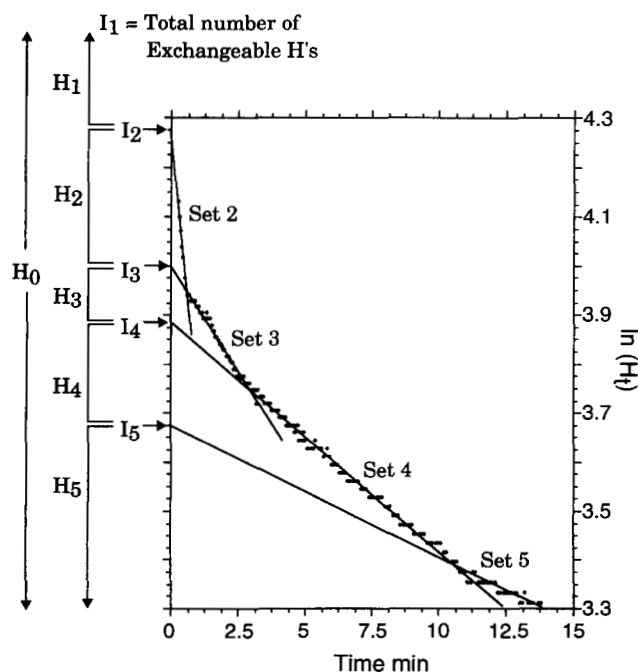


Fig. 6. A hypothetical data set of $\ln(H_t)$ vs. time, showing 4 linear regions (sets 2–5) and their respective y -intercepts (I_n) determined by linear regression. From the intercepts the number of hydrogens in each group (H_n) can be calculated by difference. H_0 is the total number of exchangeable hydrogens and $I_1 = \ln(H_0)$.

derwent deuterium exchange at slower rates. Two further linear segments can be assigned; H_3 , represented by $\ln(H_i) = 2.86 - 1.31t$, and H_4 , represented by $\ln(H_i) = 2.57 - 0.77t$.

The percentage of α -helical residues in the peptide can be estimated from the number of slowly exchanging hydrogens. E8C contained 25 slowly exchanging hydrogens that were assumed to be involved in i to $i - 4$ α -helical hydrogen bonds because the other exchangeable hydrogens (α NH_3^+ , CO_2H) should have exchanged very rapidly (before mass spectral detection) at pH 9.5. Because the main-chain NH groups of the first 4 residues of an α -helix cannot form i to $i - 4$ α -helical hydrogen bonds, the total number of residues in α -helical conformation should be 29 (25 + 4). The percentage of α -helical residues in peptide E8C was 94% (29/31). By the same reasoning, peptide E8B had 8–9 slowly exchanging hydrogens, 12–13 α -helical residues, and 40% α -helicity. Similarly, peptide E8A had 4 slowly exchanging hydrogens, 8 α -helical residues, and 26% α -helicity.

Comparison of the CD and ESI-MS results

CD spectroscopy measures the time-independent average α -helicity of the population of peptide conformations. In contrast, ESI-MS deuterium exchange measures the time-dependent incorporation of deuteriums, which provides information on the kinetic stability of the α -helix that is not obtainable from CD spectra. Because ESI-MS measures the deuterium exchange rate for a set of slowly exchanging hydrogens, a direct comparison between the 2 methods is possible when the hydrogens not involved in hydrogen bonds exchange much faster than those that are involved in hydrogen bonds. This situation occurred for peptides E8A, E8B, and E8C at pH 9.5, as evidenced by the fact that their α -helicities as measured by deuterium exchange ESI-MS (26%, 40%, and 94%, respectively) agreed well with their α -helicities as measured by CD spectroscopy (17%, 34%, and 98%, respectively).

β -Sheet proteins

Design

The betabellins are a set of synthetic proteins designed to fold into a β -barrel (Richardson & Richardson, 1987; Richardson et al., 1992). Betabellin 12 (McClain et al., 1992; Yan, 1994) and betabellin 14 (Yan & Erickson, 1994a, 1994b) were each synthesized as a single 32-residue peptide chain (Fig. 1) that would fold into an antiparallel β -sheet consisting of four 6-residue β -strands connected by three 2-residue β -turns (Fig. 7). The 6 residues of each β -strand have an alternating pattern of hydrophobic and hydrophilic residues so that the β -sheet has a hydrophobic face and a hydrophilic face. Two β -sheets were designed to pack their hydrophobic faces against each other in water to form a non-covalent β -barrel dimer. Betabellin 12S and 14S refer to the structures of the peptide chains in water. Two other chains were synthesized as a covalent dimer by air oxidation of their Cys 21 thiol groups to form a disulfide bond. Betabellin 12D and 14D refer to the structures of the disulfide-bridged double-chain dimers in water.

The betabellin target structure requires that both β -sheets have the normal right-handed twist and that the 6 β -turns between the β -strands should be type-I' β -turns (Richardson & Richard-

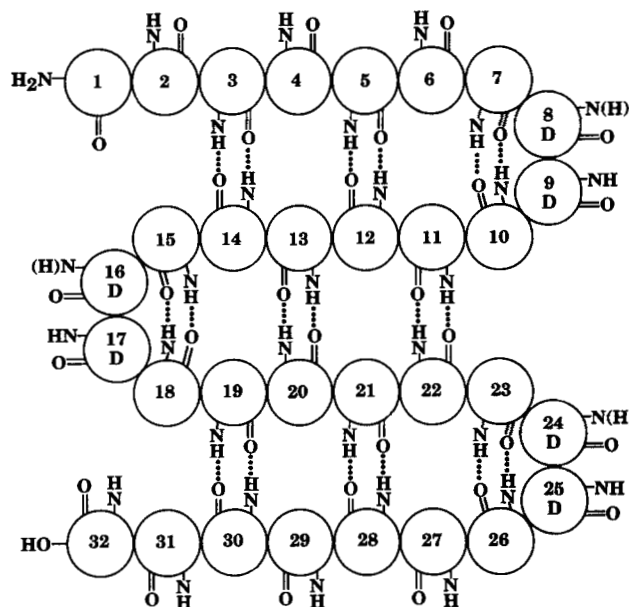


Fig. 7. Predicted β -sheet structure of betabellins, showing the expected positions of backbone amide hydrogen bonds. The hydrogens in parentheses (positions 8, 16, and 24) are only present in betabellin 14S and 14D. In betabellin 12S and 12D, these positions are proline residues.

son, 1987; Richardson et al., 1992). Betabellin 12 was designed with 3 D-Pro-D-Asp segments per chain to favor the formation of type-I' β -turns at the desired locations (McClain et al., 1992; Richardson et al., 1992). Molecular dynamics simulations have indicated that a D,D-dipeptide segment favors formation of a type-I' β -turn (Yan et al., 1993; Tropsha et al., 1994). Therefore, betabellin 14 was designed with a D-Ala-D-Lys and 2 D-Lys-D-Ala segments per chain to favor the formation of type-I' β -turns between the β -strands (Yan & Erickson, 1994a, 1994b). Several other residue changes were made to increase water solubility and decrease the isoelectric point, so that betabellin 14 shared only 15 of 32 residues with betabellin 12 (Fig. 1).

CD spectroscopy

By the criterion of CD spectroscopy, betabellin 14S was disordered in water and in 10% $\text{CH}_3\text{OH}/0.5\%$ $\text{CH}_3\text{CO}_2\text{H}$ (pH 3.8), and betabellins 12S, 12D, and 14D contained substantial β -sheet but no α -helical structure (McClain et al., 1992; Yan, 1994; Yan & Erickson, 1994a, 1994b). The CD spectra of these latter 3 proteins displayed a minimum at 217 nm, which is diagnostic of β -sheet structure. The chemical denaturation of betabellins 12S, 12D, and 14D with increasing concentration of guanidinium chloride was monitored by the change in mean ellipticity per residue at 217 nm. The concentration of guanidinium chloride that produced half denaturation was 0.4 M for betabellin 14D, 1.6 M for betabellin 12S, and 2.4 M for betabellin 12D. The elevated temperature that produced half denaturation was 58 °C for betabellin 14D, 65 °C for betabellin 12S, and 73 °C for betabellin 12D (Yan, 1994; Yan & Erickson, 1994b). Thus, the relative stability these 4 betabellins to denaturation with increasing temperature or guanidinium chloride concentration was 12D > 12S > 14D > 14S.

Electrospray ionization mass spectrometry

Lyophilized samples of betabellins 12S and 12D were separately dissolved in 10% CH₃OH/0.5% CH₃CO₂H (pH 3.8). Because these polypeptides contained several basic residues, positive ionization was used for their mass spectral analysis. The ESI mass spectrum of the 32-residue chain of betabellin 12S showed peaks for the +2 (m/z 1,683.1), +3 (m/z 1,122.2), and +4 (m/z 841.7) charge states (Fig. 8A), giving a measured molecular mass for the uncharged betabellin-12 chain of 3,363.5 Da, consistent with the calculated average mass (3,363.8 Da). The mass spectrum of the 64-residue disulfide-bridged dimer 12D displayed some peaks having similar m/z ratios but corresponding to different charge states: +4 (m/z 1,682.5), +5 (m/z 1,346.0), +6 (m/z 1,121.7), +7 (m/z 961.8), and +8 (m/z 841.8) (Fig. 8B). The molecular mass of betabellin 12D (6,725.1 Da) corresponded to 2 uncharged betabellin-12 chains minus the 2 hydrogens lost during formation of the disulfide bond. The ESI mass spectrum of betabellin 14S showed peaks for the +2 (m/z 1,726.4), +3 (m/z 1,151.2), +4 (m/z 863.6), and +5 (m/z 691.2) charge states, giving a measured molecular mass of 3,450.8 Da, consistent with the calculated average mass (3,451.0 Da). Likewise, the ESI mass spectrum of betabellin 14D showed peaks for the +5 (m/z 1,381.2), +6 (m/z 1,151.0), +7 (m/z 986.8), +8 (m/z 863.6), +9 (m/z 767.6), and +10 (m/z 690.8) charge states, giving a measured molecular mass of 6,899.9 Da, consistent with the calculated average mass (6,900.0 Da).

Observed sets of exchanging hydrogens

A lyophilized sample of betabellin 12S, 12D, 14S, or 14D was dissolved in 10% CD₃OD/0.5% CD₃CO₂D in D₂O (pD 3.8) and the increase in its molecular mass with time was immediately monitored by ESI-MS through the change in the m/z of its most abundant charge state: +3 for the betabellin-12 chain (53 exchangeable hydrogens), +4 for the betabellin-14 chain (62

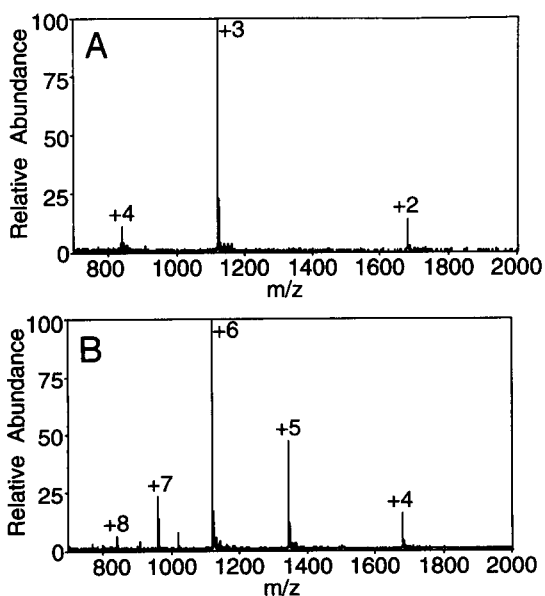


Fig. 8. ESI mass spectra of betabellins 12S (A) and 12D (B) in 10% CH₃OH/0.5% CH₃CO₂H (pH 3.8).

exchangeable hydrogens), +6 for the 12D double chain (104 exchangeable hydrogens), and +8 for the 14D double chain (122 exchangeable hydrogens).

The experiments were performed at pH 3.8, which is close to the amide exchange rate minimum (pH 3.0), thus all amides exchange on a relatively slow time scale. In addition, between pH 3 and 4, labile hydrogens on some of the side chains have similar exchange rates to the amide hydrogens. Therefore, the first linear region in Figures 9 and 10 not only represents the hydrogens involved in H-bonding but also noninteracting amide hydrogens on the backbone, side-chain amides (Asn, Gln), and some nonamide side-chain groups (Lys, His) that do not exchange rapidly.

Table 1 lists the kinetic quantities from the betabellin curves (Figs. 9, 10). For each linear segment, the negative slope k_n (the apparent first-order rate constant for set n), the y -intercept I_n (the natural logarithm of the number of exchangeable hydrogens remaining in set n and all slower exchanging sets), and r (the linear regression coefficient) are given along with $t_{1/2}$, the half-life for deuterium exchange, and k_{rel} , the relative first-order rate of deuterium exchange normalized to the rate for set 4 of betabellin 12D.

The exchange rates of the linear sets varied from $4.7 \times 10^{-2} \text{ s}^{-1}$ (14D set 2, $t_{1/2} = 0.3 \text{ min}$, $k_{rel} = 61$) to $4.3 \times 10^{-4} \text{ s}^{-1}$ (12D set 5, $t_{1/2} = 27 \text{ min}$, $k_{rel} = 0.6$), spanning a 100-fold range. The ESI-MS data were sufficiently complete that 4 linear 12D sets with k_{rel} values of 0.6, 1.0, 1.9, and 12 were distinguishable. Relative to the very slow 12D set 4 ($k_{rel} = 1$), the various sets of hydrogens can be described according to their relative exchange rates and placed into 1 of 4 categories: very fast ($k_{rel} > 300$), fast ($300 > k_{rel} > 30$), slow ($30 > k_{rel} > 3$), or very slow ($k_{rel} < 3$). In an absolute sense, the rates for the betabellins are much slower than those for the helical peptides described above. This is almost certainly an effect of the different pH values used for the 2 experiments and should not be interpreted as being related to the relative stability of α -helices and β -sheets.

Table 2 distributes the various sets of hydrogens according to their exchange rates into these 4 categories. For reference, deuterium exchange experiments monitored by NMR would predict that the intrinsic exchange rate at pH 3.8 of peptide backbone amide hydrogens (normally the slowest exchanging hydrogens) should be about $80 \times 10^{-4} \text{ s}^{-1}$ (Wüthrich, 1986), corresponding to a $k_{rel} = 10$ in our system.

Visual inspection of the exchange data from Figures 9 and 10 and Table 1 revealed that the deuterium exchange was slowest for the covalent dimer betabellin 12D, slightly faster for betabellin 12S, much faster for the covalent dimer 14D, and fastest for the disordered peptide 14S. Thus, the order of decreasing stability of the β -sheet structures of these 4 betabellins to deuterium exchange as measured by ESI-MS was the same as their order of decreasing stability to unfolding with increasing temperature or guanidinium chloride concentration (12D > 12S > 14D > 14S) as measured by CD spectroscopy.

Nearly all hydrogens of betabellin 14S exchanged with a $k_{rel} > 10$, suggesting that no hydrogen bonding is occurring in the structure. CD indicated that betabellin 14S has no recognizable secondary structure, concurring with the ESI-MS result.

Betabellin 14D showed 31 slowly exchanging hydrogens with a $k_{rel} < 8.5$. These hydrogens might be assigned to the peptide hydrogen bonds involved in forming the β -sheet secondary structure. The remaining 91 hydrogens, in the fast and very fast cat-

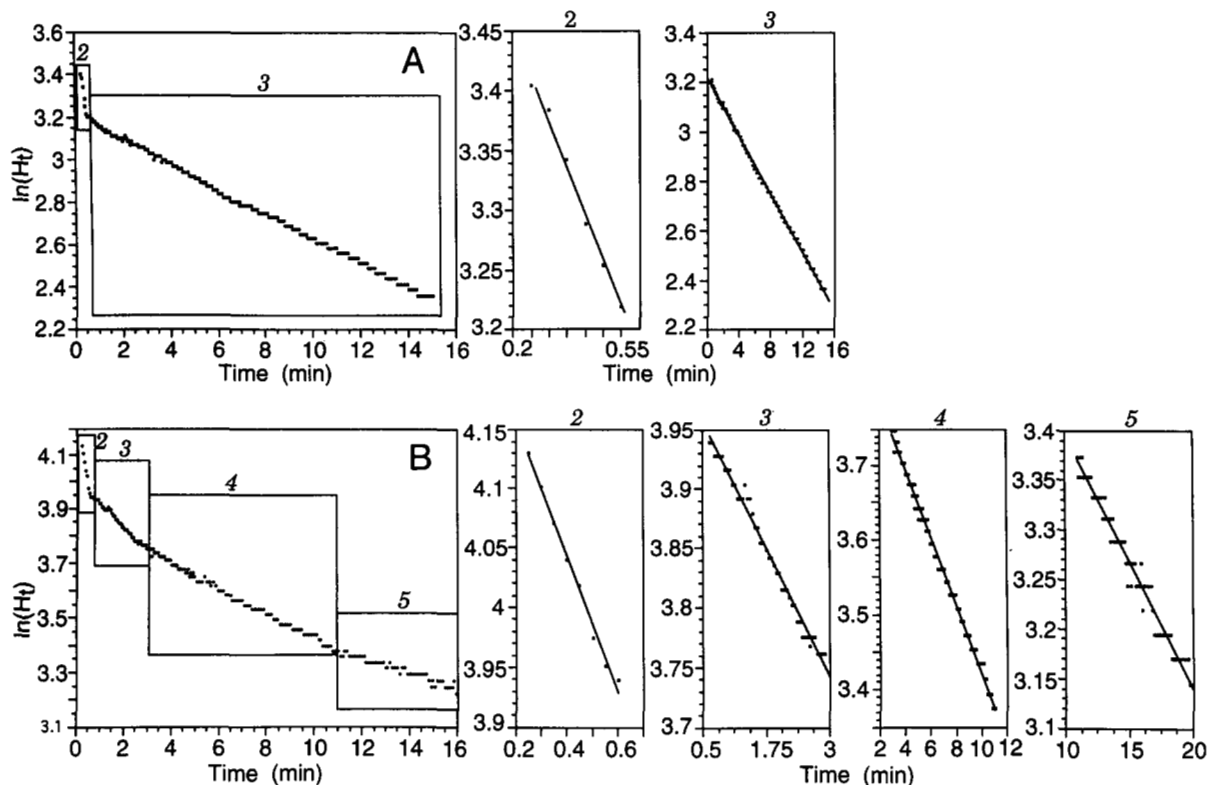


Fig. 9. Time-dependent decrease in the number of exchangeable hydrogens remaining in betabellin 12S (A) and 12D (B) following exposure to deuterated solvents. Boxed regions are expanded in panels to the right along with best-fit regression lines. Each box represents a population of hydrogens exchanging at a similar rate. Numerical data are shown in Table 1.

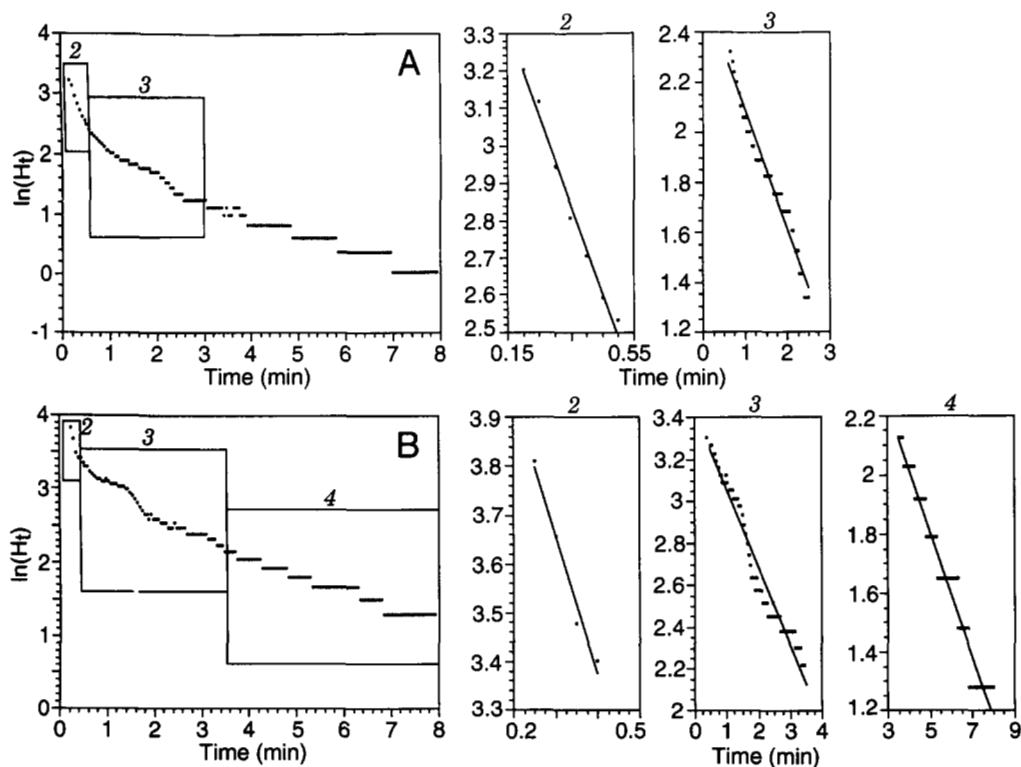


Fig. 10. Time-dependent decrease in the number of exchangeable hydrogens remaining in betabellin 14S (A) and 14D (B) following exposure to deuterated solvents. Boxed regions are expanded in panels to the right along with best-fit regression lines. Each box represents a population of hydrogens exchanging at a similar rate. Numerical data are shown in Table 1.

Table 1. Summary of the betabellin deuterium exchange data for the sets of hydrogens having similar exchange rates

Compound	<i>n</i>	Time period (min)	Slope, k_n ($\times 10^{-4} \text{ s}^{-1}$)	Relative rate, k_{rel}	<i>y</i> -Intercept	Regression coefficient, <i>r</i>	Labile H, H_n	Half-life of exchange, $t_{1/2}$ (min)
12S (Fig. 9A)	1	0–0.2	>2,300	>300			16.8 ± 0.7	<0.05
	2	0.2–0.6	120 ± 8	16	3.59 ± 0.019	0.990	11.2 ± 0.7	0.96
	3	0.6–15.0	9.73 ± 0.02	1.3	3.22 ± 0.001	0.999	14.4 ± 0.2	12.0
	4	>15	≥9.73	≤1.3	(2.36 ± 0.15)		10.6 ± 0.2	≥12.0
12D (Fig. 9B)	1	0–0.2	>2,300	>300			31.7 ± 0.5	<0.05
	2	0.2–0.6	95.0 ± 2.8	12	4.28 ± 0.007	0.995	17.6 ± 0.5	1.2
	3	0.6–3.0	14.4 ± 0.3	1.9	4.00 ± 0.003	0.994	6.2 ± 0.3	8.0
	4	3.0–11.0	7.68 ± 0.06	[1] ^a	3.88 ± 0.002	0.997	9.9 ± 0.3	15.0
	5	11.0–15.0	4.27 ± 0.07	0.6	3.65 ± 0.007	0.987	15.4 ± 0.4	27.1
	6	>15	≥4.27	≤0.6	(3.14 ± 0.014)		23.2 ± 0.3	≥27.1
14S (Fig. 10A)	1	0–0.2	>2,300	>300			22.9 ± 1.8	<0.05
	2	0.2–0.5	392 ± 25	51	3.67 ± 0.045	0.993	22.6 ± 1.9	0.29
	3	0.6–1.2	125 ± 6	16	3.81 ± 0.034	0.987	3.8 ± 0.6	0.92
	4	1.2–2.5	75.8 ± 2.4	10	2.54 ± 0.025	0.961	8.9 ± 0.4	1.51
	5	>2.5	≥75.8	≤10	(1.33 ± 0.05)		3.8 ± 0.2	≥1.51
14D (Fig. 10B)	1	0–0.2	>2,300	>300			31.7 ± 10	<0.05
	2	0.2–0.4	470 ± 50	61	4.50 ± 0.100	0.989	58.7 ± 10	0.25
	3	0.4–3.5	65.3 ± 1.6	8.5	3.45 ± 0.021	0.980	14.0 ± 0.9	1.18
	4	3.5–8.0	35.2 ± 0.7	5	2.87 ± 0.025	0.982	14.0 ± 0.6	3.28
	5	>8.0	≥35.2	≤5	(1.27 ± 0.10)		3.6 ± 0.4	≥3.28

^a The *k* for this set of protons was used to normalize the k_{rel} for all other sets.

egories, represent the side-chain hydrogens and the remaining backbone amide hydrogens.

Betabellin 14D showed slightly slower exchange than betabellin 14S: the slowly exchanging hydrogens have $k_{rel} = 5$ –8.5 for 14D, as opposed to $k_{rel} = 10$ –16 for 14S. Betabellin 14D showed considerable β -sheet structure by CD, but these ESI-MS results indicate this secondary structure is readily unfolded.

In contrast, the ESI-MS data for betabellin 12S and 12D suggest substantial kinetic stability. Betabellin 12S had 25 very slowly exchanging hydrogens with a $k_{rel} \leq 1.3$. This rate is lower than would be expected for an exposed hydrogen, and is

consistent with hydrogen bonding. Of the 28 backbone amide hydrogens in betabellin 12S, 18 should be involved in interstrand hydrogen bonds (Fig. 7) and the remaining 10 should be hydrogen bonding to solvent and not accessible for intramolecular hydrogen bonding. The 25 hydrogens observed to be exchanging very slowly probably include the 18 hydrogen bonded backbone amide hydrogens plus 7 side-chain hydrogens that are making intramolecular hydrogen bonds (Table 2). Similarly, betabellin 12D had 54 very slowly exchanging hydrogens with a $k_{rel} \leq 1.9$, which probably include the 36 backbone amide hydrogens making intrachain hydrogen bonds plus 18 side-chain hydrogens (9

Table 2. Exchangeable hydrogens of 4 betabellins: Assignment of the observed sets to 4 rate categories

Category	12S 53H		12D 104H		14S 62H		14D 122H	
	No. H's	k_{rel}	No. H's	k_{rel}	No. H's	k_{rel}	No. H's	k_{rel}
Very fast: $k_{rel} > 300$	17	>300	32	>300	23	>300	32	>300
Fast: $30 < k_{rel} < 300$					22	51	59	61
Slow: $3 < k_{rel} < 30$	11	16	18	12	4	16	14	8.5
					9	10	14	5
					4	≤10	3	≤5
Very slow: $k_{rel} < 3$	14	1.3	6	1.9				
	11	≤1.3	10	[1]				
			15	0.6				
			23	≤0.6				

per chain). The 7 very slowly exchanging nonpeptide hydrogens in betabellin 12S and the 18 similar hydrogens in betabellin 12D may be due to side-chain-side-chain hydrogen bonding on the hydrophilic faces of the β -sheets.

The exchangeable hydrogens of betabellin 12S and 12D exchange either very fast or slow/very slow, but none fall in the fast category. Betabellin 12S has 17 very fast hydrogens and betabellin 12D has 16 very fast hydrogens per chain. Additionally, betabellin 12S has 36 slow/very slow exchanging hydrogens and betabellin 12D has 36 slow/very slow exchanging hydrogens per chain. The similarity of these numbers strongly suggests that these 2 betabellins are folded in the same manner. This conclusion is consistent with results from other methods such as CD and size-exclusion chromatography, which show that betabellin 12S is a noncovalent dimer (Yan, 1994).

Conclusions

Deuterium exchange monitored by ESI-MS was useful for determining the relative structural stability of α -helical peptides and β -sheet proteins. The results obtained by ESI-MS were consistent with those measured by CD spectroscopy. Mass spectrometry alone cannot be used at present to distinguish between the slowly exchanging backbone amide hydrogens of α -helices and those of β -sheets. However, the results presented here illustrate how different sets of slowly exchanging hydrogens can be kinetically defined, how the number of hydrogens and the apparent first-order rate constant for each set can be determined, and how, in favorable cases, the relative amount of secondary structure (α -helicity) can be calculated from ESI-MS data. Hydrogen NMR spectrometry is a very powerful technique for measuring the deuterium exchange of individual hydrogens, but it requires a large amount of sample (3–100 mg), a long analysis time (6–48 h), and chemical quenching of the exchange reaction by rapid cooling to 0 °C and lowering the pH to 1.5. In contrast, monitoring deuterium exchange by ESI-MS requires much less sample (1–50 μ g), much shorter analysis time (10–90 min), and no chemical quenching. Work is in progress to explore the usefulness of this technique in determining the location of intramolecular regions that are relatively stable to deuterium exchange, the exchange rates of individual backbone amide hydrogens, and the effects of ligand-protein or protein-protein interactions on deuterium exchange.

Materials and methods

Materials

The following deuterated solvents were purchased from Cambridge Isotopes (Woburn, Massachusetts): D₂O, CF₃CD₂OD, CD₃OD, and ND₄OD (each 99.9% D) and CD₃CO₂D (99.8% D). The synthetic peptides and proteins were assembled automatically using the solid-phase method of Russ Henry at the NIEHS-UNCCH Protein Chemistry Laboratory from Fmoc-protected amino acids. These peptides and proteins were then purified by reversed-phase HPLC and were characterized by amino acid analysis, CD spectroscopy, Edman sequencing, and ESI-MS (McClain et al., 1992; Melton et al., 1994; Yan & Erickson, 1994a).

Circular dichroic spectroscopy

CD spectra were obtained with an AVIV model 62DS CD spectrophotometer using quartz cells with a 1-mm pathlength. The measured ellipticity data were corrected by a blank, averaged, and converted into mean ellipticity per residue ($[\theta]$) by dividing by bCn , where b was the pathlength of the cell, C was the molar concentration of peptide or protein, and n was the number of its residues. CD spectra are presented as a plot of $[\theta]$ (deg cm²/dmol) versus wavelength (nm). The α -helicity of a peptide or protein in solution was estimated by CD spectroscopy as the ratio $[\theta]_{222}/[\theta]_{\max}$, where $[\theta]_{222}$ is the observed ellipticity at 222 nm and $[\theta]_{\max}$ is the maximum theoretical ellipticity at 222 nm, which was calculated (Chen et al., 1974) as

$$[\theta]_{\max} = -39,500[1 - (2.57/n)] \text{ deg cm}^2/\text{dmol}.$$

Electrospray ionization mass spectrometry

ESI mass spectra were collected with a Sciex model API-III mass spectrometer (Sciex, Thornhill, Ontario) in either the positive-ion or negative-ion mode. A solution of the sample was infused into the mass spectrometer with a Harvard model 22 syringe pump (Harvard Apparatus, South Natick, Massachusetts). In the positive-ion mode, the ion-spray needle was maintained at 5,300 V and the orifice potential was held at 80 V. In the negative-ion mode, the needle was kept at -4,800 V and the orifice potential at -80 V. The enclosed ionization chamber of the mass spectrometer was kept at room temperature and atmospheric pressure. It was constantly flushed with nitrogen at 8 L/min to prevent the back exchange of deuteriums by hydrogens upon reaction with H₂O in the laboratory air. Under these conditions, exchange of hydrogen by deuterium occurred only in the solution phase, and back exchange of deuterium by hydrogen was negligible during ESI-MS analysis in the gas phase.

Each MS sample was lyophilized to dryness to minimize the presence of H₂O. In a typical deuterium exchange experiment, the solid peptide or protein was quickly dissolved in sufficient deuterated solvent to produce a final concentration of 5 μ M. This solution was immediately infused into the ionization chamber of the mass spectrometer at a rate of 2 μ L/min. Collection of the initial MS data was begun as quickly as possible, usually within 10–20 s of dissolution. A small mass range (25–30 Da) containing a selected charge state of the molecular ion was scanned repetitively using a step size of 0.1 or 0.2 Da, a dwell time of 10 ms, and a total scan time of 1.2–3 s. The (uncharged) molecular mass was calculated from the measured m/z of a known charge state and was plotted against time. At each time point, the increase in molecular mass over that of the nondeuterated molecule provided the average number of deuteriums incorporated into the peptide or protein. The nominal pD of a portion of the solution of peptide or protein was measured with a standard glass electrode previously calibrated with aqueous solutions.

Acknowledgments

This study was supported in part by NIH grants GM 42031 and HL 45100 (B.W.E.).

References

- Brandt P, Woodward C. 1987. Hydrogen exchange kinetics of bovine pancreatic trypsin inhibitor β -sheet protons in trypsin-bovine pancreatic inhibitor, trypsinogen-bovine pancreatic trypsin inhibitor, and trypsinogen-isoleucylvaline-bovine pancreatic trypsin inhibitor. *Biochemistry* 26:3156-3162.
- Bycroft M, Matouschek A, Kellis JT, Serrano L, Fersht AR. 1990. Detection and characterization of a folding intermediate in barnase by NMR. *Nature* 346:488-490.
- Chen YH, Yang JT, Chau KH. 1974. Determination of the helix and β -form of proteins in aqueous solution by circular dichroism. *Biochemistry* 13:3350-3359.
- Chou PY, Fasman GD. 1974. Prediction of protein conformation. *Biochemistry* 13:211-222.
- Covey TR, Bonner RF, Shushan BI, Henion J. 1988. The determination of protein, oligonucleotide and peptide molecular weights by ion-spray mass spectrometry. *Rapid Commun Mass Spectrom* 2:249-256.
- Creighton TE. 1984. *Protein structures and molecular properties*. New York: Freeman. pp 265-333.
- Creighton TE. 1990. Protein folding. *Biochem J* 270:1-16.
- Dobson CM, Evans PA. 1988. Trapping folding intermediates. *Nature* 335:666-667.
- Englander SW, Downer NW, Teitelbaum H. 1972. Hydrogen exchange. *Annu Rev Biochem* 41:903-924.
- Englander SW, Kallenback NR. 1984. Hydrogen exchange and structural dynamics of proteins and nucleic acids. *Q Rev Biophys* 16:521-655.
- Englander SW, Mayne L. 1992. Protein folding studied using hydrogen-exchange labeling and two-dimensional NMR. *Annu Rev Biophys Biomol Struct* 21:243-265.
- Fenn JB, Mann M, Meng CK, Wong SK, Whitehouse CM. 1990. Electrospray ionization—Principles and practice. *Mass Spectrom Rev* 9:37-70.
- Hodges RS, Semchuk PD, Taneja AK, Kay CM, Parker JMR, Mant CT. 1988. Protein design using model synthetic peptides. *Pept Res* 1:19-30.
- Hvidt A, Nielsen SO. 1966. Hydrogen exchange in proteins. *Adv Protein Chem* 21:287-386.
- Jeng MF, Englander SW, Elove GA, Wand AJ, Roder H. 1990. Structural description of acid-denatured cytochrome *c* by hydrogen exchange and 2D NMR. *Biochemistry* 29:10433-10437.
- Katta V, Chait BT. 1991. Conformational changes in proteins probed by hydrogen-exchange electrospray-ionization mass spectrometry. *Rapid Commun Mass Spectrom* 5:214-217.
- Kim PS, Baldwin RL. 1982. Influence of charge on the rate of amide proton exchange. *Biochemistry* 21:1-5.
- LeBlanc JCY, Beuchemin D, Siu KWM, Guevremont R, Berman SS. 1991. Thermal denaturation of some proteins and its effect on their electrospray mass spectra. *Org Mass Spectrom* 26:831-839.
- Mathew JB, Richards FM. 1983. The pH dependence of hydrogen exchange in proteins. *J Biol Chem* 258:3039-3044.
- Mayne L, Paterson Y, Cerasoli D, Englander SW. 1992. Effect of antibody binding on protein motions studied by hydrogen-exchange labeling and two dimensional NMR. *Biochemistry* 31:10678-10685.
- McClain RD, Yan Y, Williams RW, Donlan ME, Erickson BW. 1992. Protein engineering of betabellin 12. In: Smith JA, Rivier JE, eds. *Peptides: Chemistry and biology*. Leiden, The Netherlands: ESCOM Science. pp 364-365.
- Melton LG, Church FC, Erickson BW. 1994. Designed polyanionic coiled-coil proteins: Acceleration of heparin-cofactor II inhibition of thrombin. *Int J Pept Protein Res*. Forthcoming.
- Miranker A, Robinson CV, Radford SE, Aplin RT, Dobson CM. 1993. Detection of transient protein folding populations by mass spectrometry. *Science* 262:896-900.
- Mirza UA, Cohen SL, Chait BT. 1993. Heat-induced conformational changes in proteins studied by electrospray ionization mass spectrometry. *Anal Chem* 65:1-6.
- Molday RS, Englander SW, Kallen RG. 1972. Primary structure effects on peptide group hydrogen exchange. *Biochemistry* 11:150-158.
- Paterson Y, Englander SW, Roder H. 1990. An antibody binding site on cytochrome *c* defined by hydrogen exchange and two-dimensional NMR. *Science* 249:755-759.
- Perrin CL, Lollo CP. 1984. NMR site-to-site rate constants and the mechanisms of acid-catalyzed proton exchange in secondary amides. *J Am Chem Soc* 106:2754-2757.
- Richardson JS, Richardson DC. 1987. Some design principles: Betabellin. In: Oxender DL, Fox CF, eds. *Protein engineering*. New York: Liss. pp 149-163.
- Richardson JS, Richardson DC, Tweedy NB, Gernert KM, Quinn TP, Hecht MH, Erickson BW, Yan Y, McClain RD, Donlan ME, Surles MC. 1992. Looking at proteins: Representations, folding, packing, and design. *Biochem J* 63:1186-1209.
- Roder H, Wagner G, Wüthrich K. 1985. Individual amide proton exchange rates in thermally unfolded basic pancreatic trypsin inhibitor. *Biochemistry* 24:7407-7411.
- Rohl CA, Scholtz JM, York EJ, Stewart JM, Baldwin RL. 1992. Kinetics of amide proton exchange in helical peptides of varying chain lengths. Interpretation by the Lifson-Roig equation. *Biochemistry* 31:1263-1269.
- Rosa JJ, Richards FM. 1979. An experimental procedure for increasing the structural resolution of chemical hydrogen-exchange measurements on proteins: Application to ribonuclease S peptide. *J Mol Biol* 133:399-416.
- Stevenson CL, Anderegg RJ, Borchardt RT. 1993. Probing helical content of growth hormone releasing factor analogs using electrospray ionization mass spectrometry. *J Am Soc Mass Spectrom* 4:646-651.
- Thevenon-Emeric G, Kozlowski J, Zhang Z, Smith DL. 1992. Determination of amide hydrogen exchange rates in peptides by mass spectrometry. *Anal Chem* 64:2456-2458.
- Tropsha A, Yan Y, Schneider SE, Li L, Erickson BW. 1994. Relative free energies of folding and refolding for model secondary structure elements in aqueous solution. In: Hodges RS, Smith JA, eds. *Peptides: Chemistry, structure & biology*. Leiden, The Netherlands: ESCOM Science. pp 883-885.
- Wagner DS, Anderegg RJ. 1994. Conformation of cytochrome *c* studied by deuterium exchange electrospray ionization mass spectrometry. *Anal Chem* 66:706-711.
- Wagner G, Wüthrich K. 1982. Amide proton exchange and surface conformation of the basic pancreatic trypsin inhibitor in solution. *J Mol Biol* 160:343-361.
- Woodward CK, Hilton BD. 1979. Hydrogen exchange kinetics and internal motions in proteins and nucleic acids. *Annu Rev Biophys Bioeng* 8:99-127.
- Woodward CK, Simon I, Tuchsens E. 1982. Hydrogen exchange and the dynamic structure of proteins. *Mol Cell Biochem* 48:135-160.
- Wüthrich K. 1986. *NMR of proteins and nucleic acids*. New York: Wiley-Interscience.
- Yan Y. 1994. Synthesis of five betabellins, nongenetic beta proteins [dissertation]. Chapel Hill: University of North Carolina.
- Yan Y, Erickson BW. 1994a. Synthesis of betabellin 14, a 64-residue nongenetic beta protein. In: Hodges RS, Smith JA, eds. *Peptides: Chemistry, structure & biology*. Leiden, The Netherlands: ESCOM Science. pp 1027-1029.
- Yan Y, Erickson BW. 1994b. Engineering of betabellin 14D: Disulfide-induced folding of a β -sheet protein. *Protein Sci* 3:1069-1073.
- Yan Y, McClain RD, Williams RW, Donlan ME, Wagner DS, Anderegg RJ, Richardson JS, Richardson DC, Erickson BW. 1994b. Engineering of betabellins 12S and 12D, two 64-residue nongenetic beta proteins. *Proc Natl Acad Sci USA*. Forthcoming.
- Yan Y, Tropsha A, Hermans J, Erickson BW. 1993. Free energies for refolding of the common beta turn into the inverse-common beta turn: Simulation of the role of D/L chirality. *Proc Natl Acad Sci USA* 90:7898-7902.
- Zhang Z, Smith DL. 1993. Determination of amide hydrogen exchange by mass spectrometry: A new tool for protein structure elucidation. *Protein Sci* 2:522-531.